Cite as: L. Cui *et al.*, *Science* 10.1126/science.aam6622 (2017).

Quantized thermal transport in single-atom junctions

Longji Cui,[1]* Wonho Jeong,[1]* Sunghoon Hur,[1] Manuel Matt,[2] Jan C. Klöckner,[2] Fabian Pauly,[2] Peter Nielaba,[2] Juan Carlos Cuevas,[3]† Edgar Meyhofer,[1]† Pramod Reddy[1,4]†

[1]Department of Mechanical Engineering, University of Michigan, Ann Arbor, MI 48109, USA. [2]Department of Physics, University of Konstanz, D-78457 Konstanz, Germany. [3]Departamento de Física Teórica de la Materia Condensada and Condensed Matter Physics Center (IFIMAC), Universidad Autónoma de Madrid, Madrid 28049, Spain. [4]Department of Materials Science and Engineering, University of Michigan, Ann Arbor, MI, 48109, USA.

*These authors contributed equally to this work.

†Corresponding authors. Email: juancarlos.cuevas@uam.es (J.C.C.); meyhofer@umich.edu (E.M.); pramodr@umich.edu (P.R.)

Thermal transport in individual atomic junctions and chains is of great fundamental interest due to unique quantum effects expected to arise in them. Here, by employing novel, custom-fabricated, picowatt-resolution calorimetric scanning probes, we measure the thermal conductance of gold and platinum metallic wires down to single-atom junctions. Our work reveals that the thermal conductance of gold single atom junctions is quantized at room temperature and shows that the Wiedemann-Franz law relating thermal and electrical conductance is satisfied even in single-atom contacts. Furthermore, we quantitatively explain our experimental results within the Landauer picture for quantum thermal transport. The experimental techniques reported here will enable thermal transport studies in atomic and molecular chains, which is key to investigating numerous fundamental issues that have remained experimentally inaccessible.

The study of thermal transport at the nanoscale is of critical importance for the development of novel nanoelectronic devices and holds promise to unravel quantum phenomena that have no classical analogs (*1*–*3*). In the context of nanoscale devices, metallic atomic-size contacts (*4*) and single-molecule junctions (*5*) represent the ultimate limit of miniaturization and have emerged as paradigmatic systems revealing novel quantum effects related to charge and energy transport. For instance, transport properties of atomic-scale systems such as electrical conductance (*6*), shot noise (*7*, *8*), thermopower (*9*–*11*) and Joule heating (*12*) are completely dominated by quantum effects, even at room temperature. Therefore, they drastically differ from those of macroscale devices. Unfortunately, the experimental study of thermal transport in these systems constitutes a formidable challenge and has remained elusive to date in spite of its fundamental interest (*13*).

Probing thermal transport in junctions of atomic dimensions is crucial for understanding the ultimate quantum limits of energy transport. These limits have been explored in a variety of microdevices (*14*–*18*) where it has been shown that, irrespective of the nature of the carriers (phonons, photons or electrons), heat is ultimately transported via discrete channels. The maximum contribution per channel to the thermal conductance is equal to the universal thermal conductance quantum $G_{0,\mathrm{Th}} = \pi^2 k_B^2 T / 3h$, where k_B is the Boltzmann constant, T is the absolute temperature and h is the Planck's constant. However, observations of quantum thermal transport in micro-scale devices were only possible at sub-Kelvin temperatures and other attempts at higher temperature regimes have yielded inconclusive results (*19*).

The energy level spacing in metallic contacts of atomic-size is of the order of electronvolts, i.e., much larger than thermal energy, therefore these junctions offer a unique opportunity to explore whether thermal transport can still be quantized at room temperature. However, probing thermal transport in atomic junctions is challenging due to technical obstacles in reproducibly creating stable atomic junctions, while measuring the miniscule heat currents flowing through the atomic chains. We present an experimental platform that allows us to measure the thermal conductance of metallic wires down to the single-atom limit. With this technique we were able to observe quantized thermal transport at room temperature. Specifically, we developed an approach that employs custom-fabricated calorimetric scanning thermal microscopy (C-SThM; Fig. 1) probes, which feature a very large thermal resistance (R_P ~ 1.3 × 10^6 K/W) and high resolution Pt thermometers with temperature resolution ($\Delta T_{\min}$) of ~0.6 mK in a 10 Hz bandwidth (*20*–*22*). These characteristics enable thermal conductance measurements with ~25 pW/K resolution, when a temperature bias of ~20 K is applied across atomic junctions. We achieved the large thermal resistance by incorporating long, "T" shaped beams with a small cross-sectional area, which also enable a very high stiffness (>10^4 N/m in the normal direction) (*20*). Both these features are critical for accomplishing atomic junction thermal measurements.

The C-SThM probes also feature a sharp metallic tip that we coated with Au or Pt, but can also be coated with other metals (*20*).

Our strategy for quantitatively measuring the thermal conductance of atomic junctions is depicted in Fig. 1A. We heated the Au substrate to a temperature T_S = 315 K, while the probe is connected to a thermal reservoir at T_P = 295 K. We then displaced the probe toward the heated substrate by piezoelectric actuation until we reached an electrical conductance of $4G_0$, with $G_0 = 2e^2/h \approx (12.9\ \text{k}\Omega)^{-1}$ being the electrical conductance quantum. This electrical conductance signals the formation of a Au-Au contact involving several atoms as established by past work (*4*). We measured the probe-substrate electrical conductance by applying a small sinusoidal voltage bias of amplitude 1 mV at a frequency of 10 kHz and recording the amplitude of the resultant electric current via a lock-in amplifier (*20*). Once we reached the threshold conductance, we withdrew the probe slowly from the substrate at a rate of 0.05 nm/s. During this process, the probe-substrate contact region is expected to become more constricted until it forms a single-atom wide junction, which is broken upon further withdrawal (Fig. 1B) (*23*). We concurrently performed thermal conductance measurements by continuously measuring the change in probe temperature ($\triangle T_P$) in response to heat flow (Q) through the atomic junction. We measure the probe temperature by monitoring the change in the resistance of the embedded Pt resistance thermometer via a sinusoidal electrical current of fixed amplitude (10 μA) and frequency (1 kHz) supplied to the probe while measuring the voltage drop across the resistor.

From the resistance network (Fig. 1A), we directly related the thermal conductance (G_{Th}) of the atomic junctions to $\triangle T_P$ by $G_{Th} = \triangle T_P/[R_P(T_S - T_P - \triangle T_P)]$, where R_P was 1.3×10^6 K/W (*20*). Representative thermal (red) and electrical conductance (blue) traces show that the electrical conductance decreases in discrete steps (Fig. 2A). Many of the curves exhibit preferential conductance values that occur at integer multiples of G_0 as expected from past work (*4*). The corresponding thermal conductance curves closely correlate to the electrical conductance curves. Further, several of the thermal conductance curves show steps with preferential conductances at $2\pi^2 k_B^2 T/3h$, a value that is twice the quantum of thermal conductance ($G_{0,Th}$). The factor of two here is a consequence of the spin degeneracy in electron transport and is not present in the usual definition of $G_{0,Th}$ because it was introduced in the context of phonon transport, where spin degeneracy is absent.

Past studies (*24–26*) on electrical conductance quantization established that the presence of plateaus in the conductance traces is insufficient evidence of quantization. Definitive conductance quantization requires an unbiased statistical analysis from a large data set. We obtained ~2000 consecutive electrical and thermal conductance traces with the procedure outlined above, which yielded electrical and thermal conductance histograms with clear peaks at $1G_0$ and $2G_{0,Th}$, respectively (Fig. 2, C and D). The thermal conductance histogram exhibits more broadening in comparison to its electrical counterpart because the time constant for our thermal measurements (~25 ms) (*20*) is larger than that for our electrical measurements (~10 μs).

The close correlation between the thermal and electrical conductances (Fig. 2A) provides important information regarding the validity of the Wiedemann-Franz law, which relates the electronic contribution of the thermal conductance, $G_{Th,e}$, to the electrical conductance G_e via: $G_{Th,e} = L_0 T G_e$, where $L_0 = (\pi^2/3)(k_B/e)^2$ is the Lorenz number (*27*). Since this basic law was originally derived with semi-classical arguments and is approximately obeyed in macroscopic wires of standard metals (*27*), it is unclear whether it should remain valid in metallic atomic junctions where the transport mechanisms are different (*28*). To test the validity of the Wiedemann-Franz law in atomic junctions we used the data in Fig. 2A to obtain the Lorenz ratio $L/L_0 = G_{Th}/L_0 G_e T$, as a function of G_e. Here, T is the average temperature of the tip and the sample and equals 305 K. This process was repeated for each set of curves shown in Fig. 2A and the data from all the four curves was collected into a two dimensional histogram shown in Fig. 2B (*20*). It is clear from the data that the value of L/L_0 is very close to 1.

We plotted a 3D histogram created from 2000 concurrently measured electrical and thermal conductance traces without any data selection (Fig. 2E) (*20*). The histogram features a large peak corresponding to (G_0, $2G_{0,Th}$), showing that the electrical and thermal conductance quantization occurs concurrently and that the quantized state is a statistically favored atomic configuration. This close correlation is also reflected in the 2D histogram (Fig. 2F) where we computed $L/L_0 = G_{Th}/L_0 G_e T = 1.06$ as mean value from the 2000 traces (*20*). The small increase above 1.00 is primarily due to contributions from phonons to the thermal conductivity, which we estimate to add ~5 - 10% (see below). The increase in L/L_0 can also have small contributions (~10 – 20 pW/K) from near-field radiative heat transfer (*29*) and even smaller contributions from the overestimation of the thermal conductance during periods of rapid transition in the electrical conductance when the thermal response lags the electrical response.

To unambiguously identify the origin of our quantization observations we employed custom-developed methods to compute the thermal and electrical conductance of Au atomic-size contacts within the framework of the Landauer-Büttiker formalism for coherent transport. We exactly simulated the experiments via a combination of molecular dynamics (MD) (*30, 31, 11*), density functional theory (DFT)

(*32*, *33*), and non-equilibrium Green's function techniques to describe the contributions of both electrons and phonons to the thermal conductance (*20*). Our MD simulations (movies S1 to S6) show that when the electrical conductance is G_0, the geometry of the atomic junction typically corresponds to atomic "dimer" bridge geometries similar to that shown in the inset of Fig. 3A. Our DFT-based calculations (Fig. 3A) for the electrical and thermal transport for a dimer geometry show that the thermal conductance at room temperature is dominated by the electronic contribution, with phonons giving only ~4% of the total signal, which is similar to the case of bulk Au wires (*34*). We also found that the electronic contribution at room temperature in this example is $G_{Th,e} \approx 0.59$ nW/K, which is close to twice the thermal conductance quantum. The reason for this quantized thermal conductance is apparent from Fig. 3B where we show that electronic transmission is dominated by a single (spin-degenerate) conduction channel and has a value very close to 1. This fact, taken together with the smooth energy dependence of the electronic transmission around the Fermi energy (*20*), leads to excellent agreement with the Wiedemann-Franz law: $G_{Th,e} \approx L_0 T G_e \approx 2G_{0,Th}$. Therefore, we conclude that for one-atom Au junctions the observed thermal conductance quantization is intricately linked to the electronic structure of this monovalent metal.

Having established the origin of thermal conductance quantization and the small contribution of phonons, we focused on the analysis of $G_{Th,e}$ to systematically study the validity of the Wiedemann-Franz law for Au contacts of arbitrary size. For this purpose, we performed 100 simulations of the formation of Au junctions at 300 K while computing the electrical and thermal conductance for the transient geometries. We present histograms constructed from the electrical and thermal conductance traces (Fig. 3C). The electrical conductance histogram is dominated by a peak close to $1G_0$, which is due to preferential formation of one-atom thick contacts and short atomic chains (*11*). The corresponding histogram for the thermal conductance (normalized by $2G_{0,Th}$) shows a very close correlation with the electrical one. Therefore, the Wiedemann-Franz law, $G_{Th,e} \approx L_0 T G_e$ holds almost exactly, irrespective of the electrical conductance value (i.e., contact size) (Fig. 3D). Although some fine details of the experimental histograms are not reproduced, these computational results are in excellent agreement with our experiments (Fig. 2) and provide compelling evidence that the quantized thermal transport we observed corresponds to Au single-atom junctions and are not affected by surface contaminants, which are known to plague nano-gap thermal transport measurements (*29*).

The observed thermal conductance quantization in Au junctions is a direct consequence of the electronic structure of these junctions, which in turn is also responsible for the validity of the Wiedemann-Franz law. However, the opposite is not true: the validity of the Wiedemann-Franz law is a consequence of the smooth energy dependence of the electronic transmission (*35*, *36*) but this does not imply that thermal transport is quantized in all cases. For example, our simulations of the Pt atomic junctions suggest that while the electrical and thermal conductance traces show discrete steps and are in agreement with the Wiedemann-Franz law (Fig. 4A), one should not expect electrical or thermal conductance quantization (*20*). Even a single-atom contact of Pt sustains multiple conduction channels with intermediate transmissions between 0 and 1 that contribute to the transport properties (Fig. 4B), which is clearly at variance with the Au case. These additional channels, as compared to Au, originate from the contribution of *d* orbitals in Pt (*11*). Further, our simulations show that the electrical and thermal conductance histograms for Pt are rather featureless and there are no strongly preferred conductance values at room temperature (*20*).

In order to unambiguously test these predictions we performed measurements using a Pt-coated scanning probe and a Pt substrate using the same methodology we used for gold atom junctions. The measured electrical and thermal conductance traces (Fig. 4C) show plateaus. A histogram-based analysis on 100 Pt traces (Fig. 4D) revealed that the Lorenz ratio is very close to 1 and therefore obeys the Wiedemann-Franz law. However, histograms of electrical and thermal conductance traces did not reveal conductance quantization (*20*), in agreement with our computational predictions. This clearly demonstrates that thermal conductance quantization is not a universal feature of all metallic systems at room temperature.

Our work provides insights into thermal transport in atomic-size Au and Pt contacts and reveals conductance quantization at room temperature in Au atom junctions. We also establish the applicability of the Wiedemann-Franz law for analyzing thermal transport in metallic atomic-size contacts. The scanning calorimetric probes presented in this work will enable thermal transport studies in molecular junctions, one-dimensional chains of atoms and individual polymer chains, all of which have been studied theoretically and computationally for over half a century (*13*, *37*) but have not been probed experimentally due to the lack of experimental tools.

REFERENCES AND NOTES

1. E. Pop, Energy dissipation and transport in nanoscale devices. *Nano Res.* **3**, 147–169 (2010). doi:10.1007/s12274-010-1019-z
2. D. G. Cahill, P. V. Braun, G. Chen, D. R. Clarke, S. H. Fan, K. E. Goodson, P. Keblinski, W. P. King, G. D. Mahan, A. Majumdar, H. J. Maris, S. R. Phillpot, E. Pop, L. Shi, Nanoscale thermal transport. II. 2003-2012. *Appl. Phys. Rev.* **1**, 011305 (2014). doi:10.1063/1.4832615
3. J. Crossno, J. K. Shi, K. Wang, X. Liu, A. Harzheim, A. Lucas, S. Sachdev, P. Kim, T. Taniguchi, K. Watanabe, T. A. Ohki, K. C. Fong, Observation of the Dirac fluid and the breakdown of the Wiedemann-Franz law in graphene. *Science* **351**, 1058–

1061 (2016). doi:10.1126/science.aad0343 Medline
4. N. Agraït, A. L. Yeyati, J. M. van Ruitenbeek, Quantum properties of atomic-sized conductors. *Phys. Rep.* **377**, 81–279 (2003). doi:10.1016/S0370-1573(02)00633-6
5. J. C. Cuevas, E. Scheer, *Molecular Electronics: An Introduction to Theory And Experiment* (World Scientific Series in Nanoscience and Nanotechnology, World Scientific, 2010).
6. E. Scheer, N. Agraït, J. C. Cuevas, A. L. Yeyati, B. Ludoph, A. Martin-Rodero, G. R. Bollinger, J. M. van Ruitenbeek, C. Urbina, The signature of chemical valence in the electrical conduction through a single-atom contact. *Nature* **394**, 154–157 (1998). doi:10.1038/28112
7. H. E. van den Brom, J. M. van Ruitenbeek, Quantum suppression of shot noise in atom-size metallic contacts. *Phys. Rev. Lett.* **82**, 1526–1529 (1999). doi:10.1103/PhysRevLett.82.1526
8. P. J. Wheeler, J. N. Russom, K. Evans, N. S. King, D. Natelson, Shot noise suppression at room temperature in atomic-scale Au junctions. *Nano Lett.* **10**, 1287–1292 (2010). doi:10.1021/nl904052r Medline
9. B. Ludoph, J. M. van Ruitenbeek, Thermopower of atomic-size metallic contacts. *Phys. Rev. B* **59**, 12290–12293 (1999). doi:10.1103/PhysRevB.59.12290
10. P. Reddy, S. Y. Jang, R. A. Segalman, A. Majumdar, Thermoelectricity in molecular junctions. *Science* **315**, 1568–1571 (2007). doi:10.1126/science.1137149 Medline
11. C. Evangeli, M. Matt, L. Rincón-García, F. Pauly, P. Nielaba, G. Rubio-Bollinger, J. C. Cuevas, N. Agraït, Quantum thermopower of metallic atomic-size contacts at room temperature. *Nano Lett.* **15**, 1006–1011 (2015). doi:10.1021/nl503853v Medline
12. W. Lee, K. Kim, W. Jeong, L. A. Zotti, F. Pauly, J. C. Cuevas, P. Reddy, Heat dissipation in atomic-scale junctions. *Nature* **498**, 209–212 (2013). doi:10.1038/nature12183 Medline
13. Y. Dubi, M. Di Ventra, Colloquium: Heat flow and thermoelectricity in atomic and molecular junctions. *Rev. Mod. Phys.* **83**, 131–155 (2011). doi:10.1103/RevModPhys.83.131
14. K. Schwab, E. A. Henriksen, J. M. Worlock, M. L. Roukes, Measurement of the quantum of thermal conductance. *Nature* **404**, 974–977 (2000). doi:10.1038/35010065 Medline
15. O. Chiatti, J. T. Nicholls, Y. Y. Proskuryakov, N. Lumpkin, I. Farrer, D. A. Ritchie, Quantum thermal conductance of electrons in a one-dimensional wire. *Phys. Rev. Lett.* **97**, 056601 (2006). doi:10.1103/PhysRevLett.97.056601 Medline
16. M. Meschke, W. Guichard, J. P. Pekola, Single-mode heat conduction by photons. *Nature* **444**, 187–190 (2006). doi:10.1038/nature05276 Medline
17. S. Jezouin, F. D. Parmentier, A. Anthore, U. Gennser, A. Cavanna, Y. Jin, F. Pierre, Quantum limit of heat flow across a single electronic channel. *Science* **342**, 601–604 (2013). doi:10.1126/science.1241912 Medline
18. M. Partanen, K. Y. Tan, J. Govenius, R. E. Lake, M. K. Mäkelä, T. Tanttu, M. Möttönen, Quantum-limited heat conduction over macroscopic distances. *Nat. Phys.* **12**, 460–464 (2016). doi:10.1038/nphys3642 Medline
19. B. Gotsmann, M. A. Lantz, Quantized thermal transport across contacts of rough surfaces. *Nat. Mater.* **12**, 59–65 (2013). doi:10.1038/nmat3460 Medline
20. Materials and methods are available as supplementary materials.
21. S. Sadat, E. Meyhofer, P. Reddy, High resolution resistive thermometry for micro/nanoscale measurements. *Rev. Sci. Instrum.* **83**, 084902 (2012). doi:10.1063/1.4744963 Medline
22. S. Sadat, E. Meyhofer, P. Reddy, Resistance thermometry-based picowatt-resolution heat-flow calorimeter. *Appl. Phys. Lett.* **102**, 163110 (2013). doi:10.1063/1.4802239
23. B. Xu, N. J. Tao, Measurement of single-molecule resistance by repeated formation of molecular junctions. *Science* **301**, 1221–1223 (2003). doi:10.1126/science.1087481 Medline
24. L. Olesen, E. Laegsgaard, I. Stensgaard, F. Besenbacher, J. Schiotz, P. Stoltze, K. W. Jacobsen, J. K. Norskov, Quantized conductance in an atom-sized point contact. *Phys. Rev. Lett.* **72**, 2251–2254 (1994). doi:10.1103/PhysRevLett.72.2251 Medline
25. J. M. Krans, C. J. Muller, N. van der Post, F. R. Postma, A. P. Sutton, T. N. Todorov, T. N. Todorov, J. M. Van Ruitenbeek, Comment on "Quantized conductance in an atom-sized point contact". *Phys. Rev. Lett.* **74**, 2146 (1995). doi:10.1103/PhysRevLett.74.2146 Medline
26. L. Olesen, E. Laegsgaard, I. Stensgaard, F. Besenbacher, J. Schiotz, P. Stoltze, K. W. Jacobsen, J. K. Norskov, Olesen et al. reply. *Phys. Rev. Lett.* **74**, 2147 (1995). doi:10.1103/PhysRevLett.74.2147 Medline
27. N. W. Ashcroft, N. D. Mermin, *Solid State Physics* (Holt, 1976).
28. U. Sivan, Y. Imry, Multichannel Landauer formula for thermoelectric transport with application to thermopower near the mobility edge. *Phys. Rev. B* **33**, 551–558 (1986). doi:10.1103/PhysRevB.33.551 Medline
29. L. Cui, W. Jeong, V. F. Hurtado, J. Feist, F. J. García-Vidal, J. C. Cuevas, E. Meyhofer, P. Reddy, Study of radiative heat transfer in Ångström and nanometre sized gaps. *Nat. Commun.* 10.1038/ncomms14479 (2017).
30. M. Dreher, F. Pauly, J. Heurich, J. C. Cuevas, E. Scheer, P. Nielaba, Structure and conductance histogram of atomic-sized Au contacts. *Phys. Rev. B* **72**, 075435 (2005). doi:10.1103/PhysRevB.72.075435
31. C. Schirm, M. Matt, F. Pauly, J. C. Cuevas, P. Nielaba, E. Scheer, A current-driven single-atom memory. *Nat. Nanotechnol.* **8**, 645–648 (2013). doi:10.1038/nnano.2013.170 Medline
32. F. Pauly, J. K. Viljas, U. Huniar, M. Hafner, S. Wohlthat, M. Burkle, J. C. Cuevas, G. Schon, Cluster-based density-functional approach to quantum transport through molecular and atomic contacts. *New J. Phys.* **10**, 125019 (2008). doi:10.1088/1367-2630/10/12/125019
33. M. Bürkle, T. J. Hellmuth, F. Pauly, Y. Asai, First-principles calculation of the thermoelectric figure of merit for [2,2]paracyclophane-based single-molecule junctions. *Phys. Rev. B* **91**, 165419 (2015). doi:10.1103/PhysRevB.91.165419
34. A. Jain, A. J. H. McGaughey, Thermal transport by phonons and electrons in aluminum, silver, and gold from first principles. *Phys. Rev. B* **93**, 081206 (2016). doi:10.1103/PhysRevB.93.081206
35. J. P. Bergfield, C. A. Stafford, Thermoelectric signatures of coherent transport in single-molecule heterojunctions. *Nano Lett.* **9**, 3072–3076 (2009). doi:10.1021/nl901554s Medline
36. V. Balachandran, R. Bosisio, G. Benenti, Validity of the Wiedemann-Franz law in small molecular wires. *Phys. Rev. B* **86**, 035433 (2012). doi:10.1103/PhysRevB.86.035433
37. N. B. Li, J. Ren, L. Wang, G. Zhang, P. Hänggi, B. W. Li, Colloquium: Phononics: Manipulating heat flow with electronic analogs and beyond. *Rev. Mod. Phys.* **84**, 1045–1066 (2012). doi:10.1103/RevModPhys.84.1045
38. B. Song, Y. Ganjeh, S. Sadat, D. Thompson, A. Fiorino, V. Fernández-Hurtado, J. Feist, F. J. Garcia-Vidal, J. C. Cuevas, P. Reddy, E. Meyhofer, Enhancement of near-field radiative heat transfer using polar dielectric thin films. *Nat. Nanotechnol.* **10**, 253–258 (2015). doi:10.1038/nnano.2015.6 Medline
39. A. Khan, J. Philip, P. Hess, Young's modulus of silicon nitride used in scanning force microscope cantilevers. *J. Appl. Phys.* **95**, 1667–1672 (2004). doi:10.1063/1.1638886
40. L. Olesen, M. Brandbyge, M. R. Sorensen, K. W. Jacobsen, E. Lægsgaard, I. Stensgaard, F. Besenbacher, Apparent barrier height in scanning tunneling microscopy revisited. *Phys. Rev. Lett.* **76**, 1485–1488 (1996). doi:10.1103/PhysRevLett.76.1485 Medline
41. TURBOMOLE version 6.5, http://www.turbomole.com.
42. P. Deglmann, F. Furche, R. Ahlrichs, An efficient implementation of second analytical derivatives for density functional methods. *Chem. Phys. Lett.* **362**, 511–518 (2002). doi:10.1016/S0009-2614(02)01084-9
43. P. Deglmann, K. May, F. Furche, R. Ahlrichs, Nuclear second analytical derivative calculations using auxiliary basis set expansions. *Chem. Phys. Lett.* **384**, 103–107 (2004). doi:10.1016/j.cplett.2003.11.080
44. J. P. Perdew, Y. Wang, Accurate and simple analytic representation of the electron-gas correlation energy. *Phys. Rev. B* **45**, 13244–13249 (1992). doi:10.1103/PhysRevB.45.13244 Medline
45. J. P. Perdew, K. Burke, M. Ernzerhof, Generalized gradient approximation made simple. *Phys. Rev. Lett.* **77**, 3865–3868 (1996). doi:10.1103/PhysRevLett.77.3865 Medline
46. F. Weigend, R. Ahlrichs, Balanced basis sets of split valence, triple zeta valence and quadruple zeta valence quality for H to Rn: Design and assessment of accuracy. *Phys. Chem. Chem. Phys.* **7**, 3297–3305 (2005). doi:10.1039/b508541a Medline
47. F. Weigend, Accurate coulomb-fitting basis sets for H to Rn. *Phys. Chem. Chem.*

Phys. **8**, 1057–1065 (2006). doi:10.1039/b515623h Medline
48. F. Guinea, C. Tejedor, F. Flores, E. Louis, Effective two-dimensional Hamiltonian at surfaces. *Phys. Rev. B* **28**, 4397–4402 (1983). doi:10.1103/PhysRevB.28.4397
49. N. Mingo, L. Yang, Phonon transport in nanowires coated with an amorphous material: An atomistic Green's function approach. *Phys. Rev. B* **68**, 245406 (2003). doi:10.1103/PhysRevB.68.245406
50. LAMMPS Molecular Dynamics Simulator, http://lammps.sandia.gov.
51. S. Plimpton, Fast parallel algorithms for short-range molecular-dynamics. *J. Comput. Phys.* **117**, 1–19 (1995). doi:10.1006/jcph.1995.1039
52. G. J. Ackland, G. Tichy, V. Vitek, M. W. Finnis, Simple *N*-body potentials for the noble metals and nickel. *Philos. Mag. A* **56**, 735–756 (1987). doi:10.1080/01418618708204485
53. H. W. Sheng, M. J. Kramer, A. Cadien, T. Fujita, M. W. Chen, Highly optimized embedded-atom-method potentials for fourteen fcc metals. *Phys. Rev. B* **83**, 134118 (2011). doi:10.1103/PhysRevB.83.134118
54. D. Frenkel, B. Smit, *Understanding Molecular Simulation* (Academic Press, 2002).
55. M. J. Mehl, D. A. Papaconstantopoulos, *Computational Materials Science*, C. Fong, Ed. (World Scientific, 1998).
56. F. Pauly, M. Dreher, J. K. Viljas, M. Häfner, J. C. Cuevas, P. Nielaba, Theoretical analysis of the conductance histograms and structural properties of Ag, Pt, and Ni nanocontacts. *Phys. Rev. B* **74**, 235106 (2006). doi:10.1103/PhysRevB.74.235106

ACKNOWLEDGMENTS

P.R. acknowledges support from DOE-BES (award No. DE-SC0004871). P.R. and E.M. acknowledge support from the Office of Naval Research (N00014-16-1-2672) and the National Science Foundation (CBET 1235691). J.C.C. acknowledges funding from the Spanish MINECO (Contract No. FIS2014-53488-P) and thanks the German Research Foundation (DFG) and Collaborative Research Center (SFB) 767 for sponsoring his stay at the University of Konstanz as Mercator Fellow. M.M. and P.N. acknowledge funding from the SFB767 and computer time granting from the NIC and the bwHPC framework program of the State of Baden-Württemberg. J.C.K. and F.P. were financially supported by the Carl Zeiss foundation, the SFB767 of the DFG, and the Junior Professorship Program of the Ministry of Science, Research, and the Arts of the state of Baden-Württemberg. All of the data are available in the main paper and the supplementary materials.

SUPPLEMENTARY MATERIALS

www.sciencemag.org/cgi/content/full/science.aam6622/DC1
Materials and Methods
Figs. S1 to S10
References (*38*–*56*)
Movies S1 to S6

27 December 2016; accepted 6 February 2017
Published online 16 February 2017
10.1126/science.aam6622

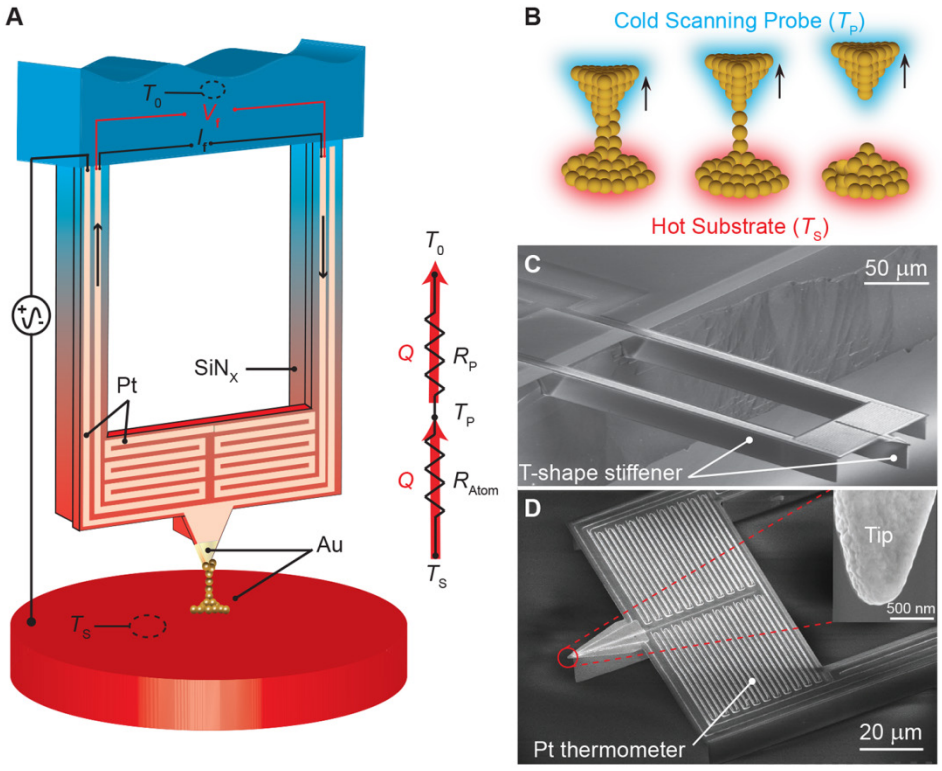

Fig. 1. Experimental set-up and SEM images of the scanning thermal probes. (**A**) Schematic of a calorimetric scanning thermal microscopy (C-SThM) probe, which is used to make atomic junctions with a heated metallic substrate. The tip and substrate coatings can be chosen to be either Au or Pt. The electrical conductance of the tip-substrate junction is monitored by applying a small sinusoidal voltage bias and measuring the resultant current. The resistance of the Pt resistance thermometer is monitored by applying a sinusoidal current (amplitude I_f) and recording the voltage output (V_f). Thermal resistance network describes the resistances of the atomic chain ($R_{Atom} = (G_{Th})^{-1}$) and the scanning probe (R_P), as well as the heat current flow (red arrow). The substrate, thermal reservoir and tip temperatures are indicated by T_S, T_0, and T_P, respectively. (**B**) Schematics of the atomic chains forming, narrowing, and breaking during the withdrawal of the probe from the heated substrate. (**C**) SEM image (side view) of a scanning probe with two long and stiff "T" shaped SiN_X beams. (**D**) SEM image (top view) of the scanning probe, featuring a Au coated tip (inset) and a serpentine Pt thermometer.

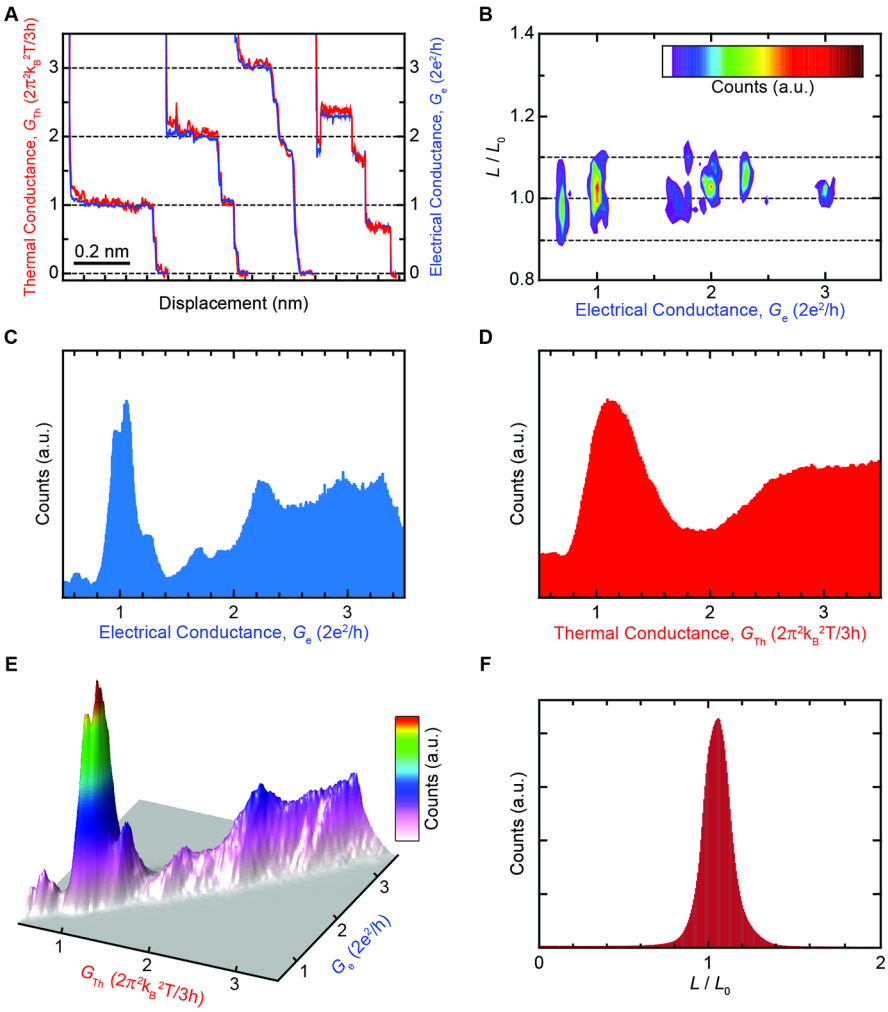

Fig. 2. Thermal conductance quantization in Au atomic junctions. (**A**) Representative traces of thermal and electrical conductances measured while reducing the transverse constriction of Au atomic junctions by displacing the Au tip of C-SThM probe away from the Au substrate. The thermal (red line) and electrical conductance (blue line) traces are plotted in units of $2\pi^2 k_B^2 T/3h$ ($2G_{0,Th}$, twice the thermal conductance quantum) and $2e^2/h$ (G_0, electrical conductance quantum), respectively. (**B**) Histogram of the ratio of the thermal conductance to electrical conductance is in good agreement with the Lorenz number (L/L_0). Color bar: number of counts increase from white to red. (**C** and **D**) Electrical and thermal conductance histograms obtained from 2000 concurrently measured electrical and thermal conductance traces (without any data selection) similar to those shown in (A). (**E**) A joint plot of the electrical and thermal conductance traces shows the tight correlation between the occurrence of electrical and thermal conductance quantization. (**F**) Analysis of the data in (C) and (D) shows that the Wiedemann-Franz law accurately predicts the thermal conductance of Au atomic junctions (the peak is at 1.06).

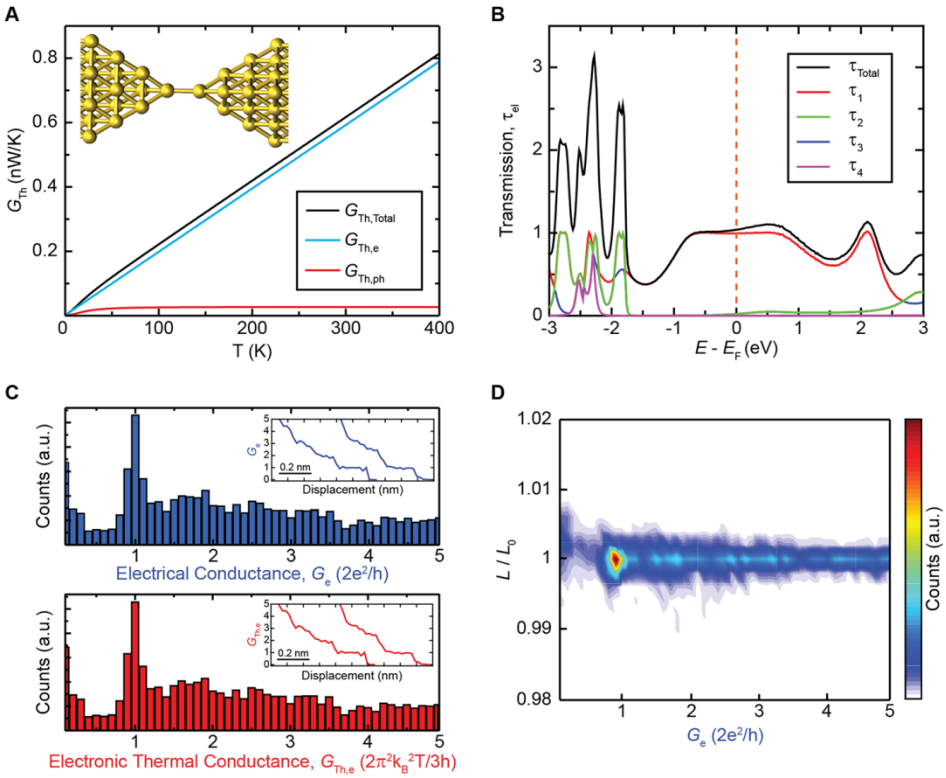

Fig. 3. Computations of thermal conductance in Au atomic junctions. (**A**) Computed thermal conductance as a function of temperature for the Au atomic junction geometry shown in the inset. The total thermal conductance (black), the electronic contribution $G_{Th,e}$ (blue), and the phononic contribution $G_{Th,ph}$ (red) to thermal conductance are shown. Notice that $G_{Th,ph}$ is almost negligible at room temperature. (**B**) The total electronic transmission and the individual electronic transmission coefficients as a function of the energy (measured with respect to the Fermi energy E_F) for the contact geometry in the inset of (A). The electronic transmission is dominated by a single (spin-degenerate) conduction channel. (**C**) Electrical and electronic thermal conductance histograms obtained from 100 MD simulations of the formation of Au atomic contacts at room temperature (insets show representative electrical and thermal conductance traces obtained from these simulations). (**D**) Lorenz ratio (L/L_0) as a function of the electrical conductance G_e of the Au contacts as obtained from the histograms in (C). Notice that the ratio is very close to one. Deviations are below 1%, which shows that the Wiedemann-Franz law is fulfilled with good accuracy, irrespective of the contact size.

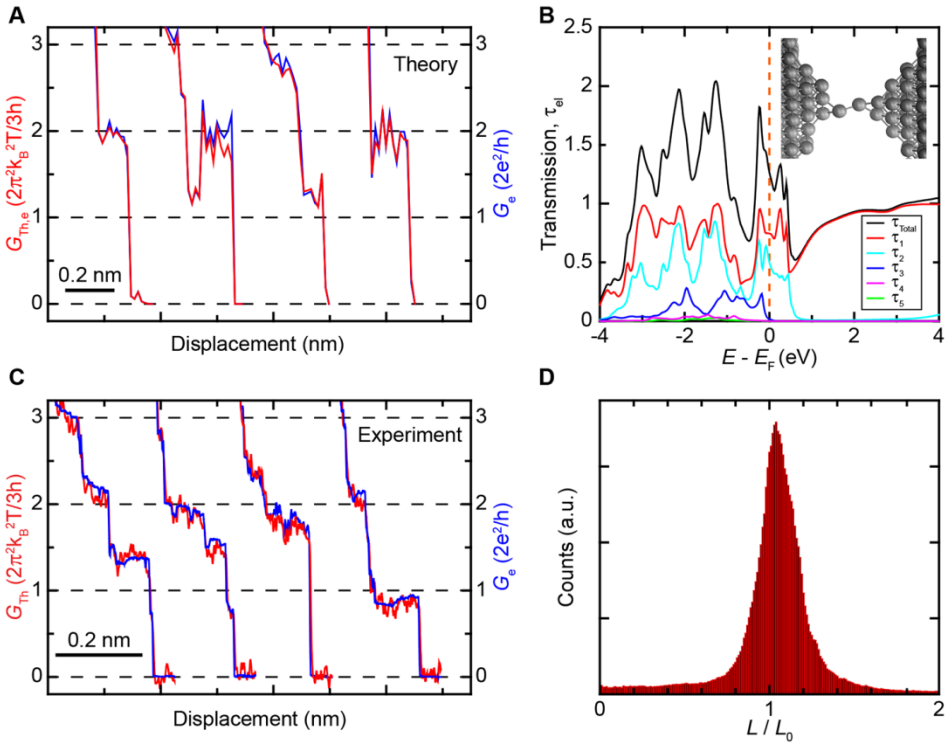

Fig. 4. Calculated and measured transport properties of Pt atomic junctions. (**A**) Representative traces of the electrical conductance (blue) and the electronic thermal conductance (red) for Pt junctions calculated by combined molecular dynamics (MD) and transport simulations. (**B**) The total electronic transmission and the individual electronic transmission coefficients as a function of the energy (measured with respect to the Fermi energy E_F) for the contact geometry shown in the inset. The electronic transmission has significant contributions from three channels at the Fermi level. Further, the transmission varies more rapidly with energy than for Au atomic junctions. (**C**) Representative measured traces of electrical (blue) and thermal (red) conductances for Pt atomic junctions show discrete steps (conductance histograms do not display electrical or thermal conductance quantization, see SM). (**D**) Histogram similar to that shown in Fig. 2F but for Pt data shows that the Wiedemann-Franz law is applicable (the peak is at 1.04). The corresponding theoretical results can be seen in fig. S10 in (*20*).

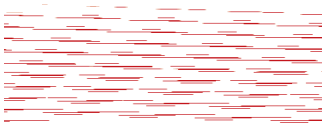

Editor's Summary

Quantized thermal transport in single-atom junctions
Longji Cui, Wonho Jeong, Sunghoon Hur, Manuel Matt, Jan C. Klöckner, Fabian Pauly, Peter Nielaba, Juan Carlos Cuevas, Edgar Meyhofer and Pramod Reddy (February 16, 2017)
published online February 16, 2017

Science (print ISSN 0036-8075; online ISSN 1095-9203) is published weekly, except the last week in December, by the American Association for the Advancement of Science, 1200 New York Avenue NW, Washington, DC 20005.